Mechanism of atomic diffusion in liquid B_2O_3: An *ab initio* molecular dynamics study

Satoshi Ohmura and Fuyuki Shimojo
Department of Physics, Kumamoto University, Kumamoto 860-8555, Japan
(Received 1 September 2008; published 23 December 2008)

The structural and bonding properties of liquid boron oxide are studied by *ab initio* molecular dynamics simulations. It is seen that, even in the liquid state, boron atoms are predominantly threefold coordinated to oxygen atoms, and most of oxygen atoms bridge two adjacent boron atoms. The neighboring atoms are connected to each other with single covalent bonds, and there exist no homopolar bonds, as in the crystalline and vitreous states. We find that a nonbridging oxygen double bonded to a twofold-coordinated boron is always involved with atomic diffusion accompanied by the rearrangement of the covalent bonds. We discuss the formation mechanism of such bond defects in detail by the population analysis.

DOI: 10.1103/PhysRevB.78.224206 PACS number(s): 61.20.Ja, 66.10.−x, 71.15.Pd

I. INTRODUCTION

Boron oxide (B_2O_3) has attracted considerable attention not only as one of the most fundamental glass-forming oxides but also as a potential material for technological and environmental applications. It is well known that the structures of crystalline and vitreous B_2O_3 consist of planar BO_3 units with threefold-coordinated boron atoms at the centers.[1,2] These triangular BO_3 units form three-dimensional networks by sharing corner oxygen atoms, i.e., each oxygen atom bridges two adjacent boron atoms with single bonds. There exist sheetlike layered structures, similar to graphite, on an intermediate length scale in the networks.[1] The structure of solid B_2O_3 is rather porous because of large empty space between layers.

Although it is known experimentally that the local coordination around each atom remains the same upon melting,[3] details of the structural and transport properties of liquid B_2O_3 are not well understood. In the liquid state, the rearrangement of the B-O covalent bonds with long-range atomic diffusion must take place. It is, however, not obvious how B-O bonds are exchanged because the chemical bonds between boron and oxygen are rather strong and stable.

While the diffusion process in the liquid state has not been clarified yet, several mechanisms of bond switching in the relaxation process in B_2O_3 glass above the glass transition temperature were proposed.[4,5] It is commonly emphasized that participation of hypervalent structures with fourfold-coordinated borons and threefold-coordinated oxygens is important in the initial stage of bond switching. In the relaxation mechanism with the usual concerted reactions,[5] two BO_4 groups are generated as an intermediate by forming two new B-O bonds between adjoining BO_3 units. When the original B-O bonds associated with the two three-coordinated oxygens are broken simultaneously, two B-O bonds are exchanged without undercoordinated atoms. On the other hand, Zyubin *et al.*[4] suggested from semiempirical quantum-chemical calculations that the formation of fragments, which involve nonbridging oxygens double bonded to twofold-coordinated borons, is the most energetically favorable in the relaxation process after the hypervalent structures with overcoordinated atoms are formed.

Since it would be difficult to clarify the diffusion mechanism in liquid B_2O_3 experimentally, theoretical studies would be needed. However, only a few papers have dealt with atomic diffusion in liquid B_2O_3,[6] and borate melts[7] theoretically so far. Diefenbacher and McMillan[6] used molecular dynamics (MD) simulations with empirical interatomic potentials to investigate the transport properties in the liquid state. They discussed the effects of pressure on the diffusivity of atoms in relation to changes in the local structure. Although they proposed a model of the diffusion process, it is unclear whether the appearance of undercoordinated atoms, such as nonbridging oxygens, is crucial for the transport properties in the liquid state.

In this paper, we report on a detailed investigation of atomic diffusion in liquid B_2O_3 by *ab initio* MD simulations with interatomic forces calculated quantum mechanically in the framework of the density-functional theory (DFT). While there have been reported several density-functional or Hartree-Fock studies for crystalline[8–11] and vitreous[12–14] B_2O_3 so far, the liquid properties have not been investigated yet based on first-principles theories. The purpose of our study is to clarify the microscopic mechanism of atomic diffusion in the liquid state from first principles. We discuss how B-O bonds are exchanged, accompanying the diffusion of atoms in detail. Such findings are important not only for understanding the equilibrium properties of liquid B_2O_3 but also for considering the glass formation process in the supercooled liquid state, in addition to the relaxation process in the vitreous state.

II. METHOD OF CALCULATION

The electronic states are calculated using the projector augmented wave (PAW) method[15,16] within the framework of the DFT in which the generalized gradient approximation (GGA) (Ref. 17) is used for the exchange-correlation energy. The plane-wave cut-off energies are 30 and 200 Ry for the electronic pseudowave functions and the pseudocharge density, respectively. The energy functional is minimized using an iterative scheme.[18,19] The Γ point is used for the Brillouin-zone sampling. As the valence electrons, we include the $2s$ and $2p$ electrons of B and O. The $1s$ electrons in the lower-energy electronic states of each atom are treated with the frozen-core approximation. We use a system of 120 (48B +72O) atoms in a cubic supercell under periodic boundary

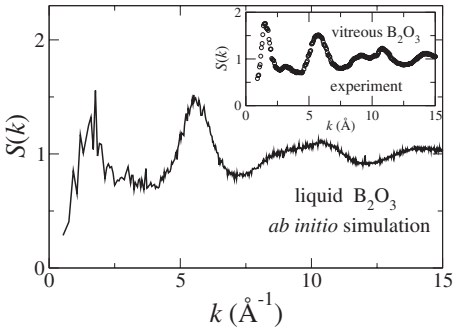

FIG. 1. Structure factor $S(k)$ of liquid B_2O_3: in the inset, the experimental $S(k)$ of vitreous B_2O_3 (Ref. 24) is shown for comparison.

conditions. Using the Nosé-Hoover thermostat technique,[20,21] the equations of motion are solved via an explicit reversible integrator[22] with a time step of $\Delta t=1.2$ fs. To obtain a liquid state, we begin by carrying out an *ab initio* MD simulation for about 5 ps at a temperature of 5000 K starting from the low-pressure crystalline polymorph B_2O_3-I.[1] The temperature is selected to be high enough to make the system reach a completely disordered state without the effects of the initial configuration. Then, we decrease the temperature of the system gradually to a target temperature of 2500 K. The number density is taken from the extrapolation of the experimental data[23] obtained up to 1500 K. The target temperature we have chosen is rather high in order to observe enough number of atomic-diffusion events to analyze the diffusion mechanism in a statistically meaningful way within a limited amount of simulation time. Note that the temperature dependence of physical quantities is not discussed in this paper and conclusions derived are independent of the selected temperature. The simulation time for averaging, 10.8 ps, is long enough to achieve good statistics.

III. RESULTS

A. Structure factor

Figure 1 shows the structure factor $S(k)$ of liquid B_2O_3, which is calculated from the partial structure factors $S_{\alpha\beta}(k)$, shown in Fig. 2, with the neutron-scattering lengths. To see whether the structure of liquid B_2O_3 is correctly reproduced or not, the structure factor $S(k)$ obtained by our simulations should be compared with experimental results. Unfortunately, we are unaware of experimental $S(k)$ for the liquid state. In the inset of Fig. 1, the experimental data obtained by neutron-diffraction measurements[24] for vitreous B_2O_3 are shown for comparison. Since the overall profile of the calculated $S(k)$ of the liquid state is consistent with the experimental $S(k)$ of the vitreous state, we believe that the structure of liquid B_2O_3 is correctly simulated by our theoretical method.

It is seen that there are clear peaks at about $k=1.6$ and 6.0 $Å^{-1}$ in the profile of $S(k)$. The peak at about $k=1.6$ $Å^{-1}$ indicates that an intermediate range correlation exits in the liquid state as well as in the vitreous state, while the peak at about $k=6.0$ $Å^{-1}$ corresponds to the short-range correlation between the nearest-neighbor atoms. Also, we see

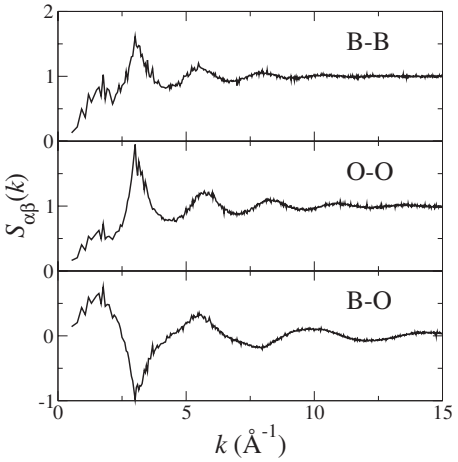

FIG. 2. Ashcroft-Langreth partial structure factors $S_{\alpha\beta}(k)$ of liquid B_2O_3.

that a hump is present at about $k=2.7$ $Å^{-1}$ between these two main peaks.

Figure 2 shows the Ashcroft-Langreth partial structure factors $S_{\alpha\beta}(k)$. It is found that all three correlations, $S_{BB}(k)$, $S_{OO}(k)$, and $S_{BO}(k)$, have peaks at about $k=1.6$ and 6.0 $Å^{-1}$ corresponding to the peaks of the total $S(k)$. We see that the profile of $S(k)$ for $k \geq 8.0$ $Å^{-1}$ is mainly formed by $S_{BO}(k)$. It is also found that the hump of $S(k)$ at about $k=2.4$ $Å^{-1}$ results from the cancellation between the peaks of $S_{BB}(k)$ and $S_{OO}(k)$ and the negative dip of $S_{BO}(k)$.

B. Pair distribution function

Figure 3 shows the partial pair distribution functions $g_{\alpha\beta}(r)$. The sharp first peak of $g_{BO}(r)$ at about 1.4 Å corresponds to the covalent bond between B and O atoms. It is seen that there exist no homopolar bonds in liquid B_2O_3 because $g_{BB}(r)$ and $g_{OO}(r)$ are zero over the range of the first peak of $g_{BO}(r)$. The first-peak positions of $g_{BB}(r)$ and $g_{OO}(r)$ are about 2.55 and 2.45 Å, respectively. This difference in peak positions reflects the fact that there is a difference between the average B-O-B and O-B-O angles. Note that this feature is also found in crystalline B_2O_3. In B_2O_3-I at ambient conditions, the average distances of B-B and O-O are 2.489 and 2.373 Å, respectively, and the average bond angles of B-O-B and O-B-O are 130.71° and 119.97°,

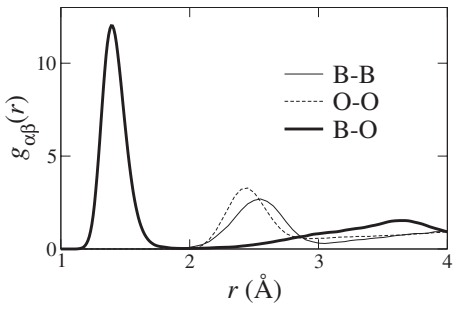

FIG. 3. Partial pair distribution functions $g_{\alpha\beta}(r)$ of liquid B_2O_3. The thick solid, thin solid, and thin dashed lines show $g_{BO}(r)$, $g_{BB}(r)$, and $g_{OO}(r)$, respectively.

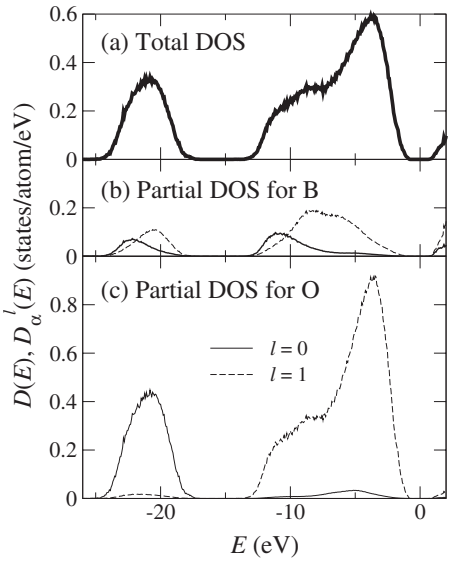

FIG. 4. (a) Total electronic DOS $D(E)$ and the partial DOS's $D_\alpha^l(E)$ for (b) α=B and (c) O in liquid B_2O_3. The solid and dashed lines in (b) and (c) show $D_\alpha^l(E)$ for l=0 and 1, respectively. The origin of energy is taken to be the Fermi level.

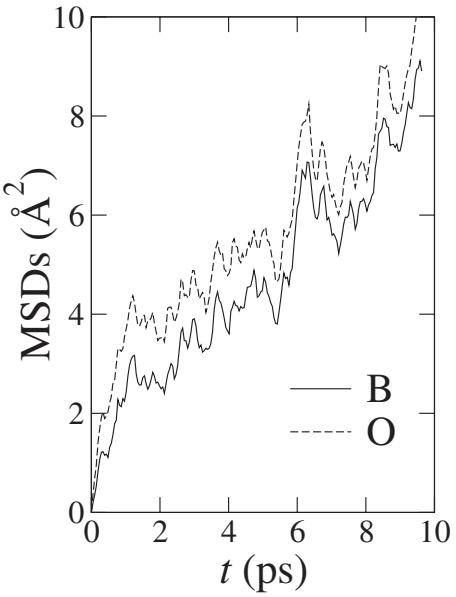

FIG. 5. MSDs in liquid B_2O_3. The solid and dashed lines show MSDs for B and O atoms, respectively.

respectively.[1] Although the atomic distances in the liquid state are naturally longer than those in the crystalline state, the trends in the relation between the atomic distances and the bond angles are the same in both states. It is seen from the integral of $g_{BO}(r)$ up to its first minimum at about 1.9 Å that the coordination numbers for B and O atoms are 3 and 2, respectively, which indicates that the triangular BO_3 units sharing corner O atoms are preserved in liquid B_2O_3.

C. Electronic density of states

Figure 4 shows the total electronic density of states (DOS), $D(E)$, and the angular momentum–dependent partial DOS, $D_\alpha^l(E)$, for α-type atoms in liquid B_2O_3. Note that $D(E)=\Sigma_\alpha c_\alpha \Sigma_l D_\alpha^l(E)$, where c_α is the number concentration of α-type atoms. In $D(E)$, there are two segments below the Fermi level (E=0) with the energy ranges of $-24\sim-18$ eV and $-12\sim-1$ eV. The overall profile of $D(E)$ in the liquid state is similar to those in crystals[9] although the latter have spiky peaks as well as a gap at about -7 eV. It is clear from $D_B^l(E)$ that the $2s$ and $2p$ states of B atoms hybridize with each other within both segments. On the other hand, almost no s-p hybridization occurs around O atoms. In the lower-energy segment, the $2s$ electrons of O atoms interact with both $2s$ and $2p$ orbitals of B atoms. Since the B-O covalent bonds are retained in the liquid state as seen from $g_{\alpha\beta}(r)$, we consider that, around each O atom, the $2p$ orbitals form two σ-type covalent bonds with neighboring B atoms and one lone-pair (LP) nonbonding state. The large peak of $D_O^{2p}(E)$ at about -4 eV originates from the LP states because there is no corresponding peak in $D_B^l(E)$. The shoulder in $D_O^{2p}(E)$ at around -10 eV comes from the hybridized state with the $2s$ and $2p$ orbitals of B atoms to form the σ-type covalent bonds.

D. Mean-square displacement

The mean-square displacements (MSDs) are shown in Fig. 5, where the solid and dashed lines show MSDs for B and O atoms, respectively. We see that both MSDs have finite slopes, which clearly indicates that a liquid state is reproduced by our simulation. It is found that O atoms diffuse faster than B atoms for short time $t<1$ ps, the reason of which is that the number of atoms bonded to one O atom is smaller than that bonded to one B atom, and therefore O atoms are more mobile in a short range. On the other hand, the long-range diffusivities are almost the same for both atoms.

E. Mechanism of atomic diffusion

As seen in Secs. III A and III D, B atoms are mainly coordinated to three O atoms, and almost all O atoms bridge two adjacent B atoms as in the crystalline phase even though atoms diffuse in the liquid state. It is obvious from the sharp first peak of $g_{BO}(r)$ and the profile of $D_\alpha^l(E)$ that the covalent bonds between B and O atoms are preserved in liquid B_2O_3. These results are in good agreement with the recent experimental observations.[3] However, it is unclear how B-O bonds are exchanged with the diffusion of atoms in the liquid state while retaining the covalent bonds. To clarify the mechanism of atomic diffusion, we investigate the time evolution of bonding nature by utilizing the population analysis.[25,26] The bond-overlap populations, which give a semiquantitative estimate of the strength of the covalentlike bonding between atoms, are calculated as a function of time.

We find that one nonbridging O atom double bonded to a twofold-coordinated B atom is always involved with atomic diffusion accompanied by the B-O bond switching. A typical example of the generation of a nonbridging oxygen is shown in Fig. 6, where the time evolution of the bond-overlap populations associated with the B and O atoms of interest is displayed with snapshots of atomic configurations. In the atomic configuration at 0.01 ps (the bottom panel of Fig. 6), all B and O atoms displayed are threefold- and twofold-

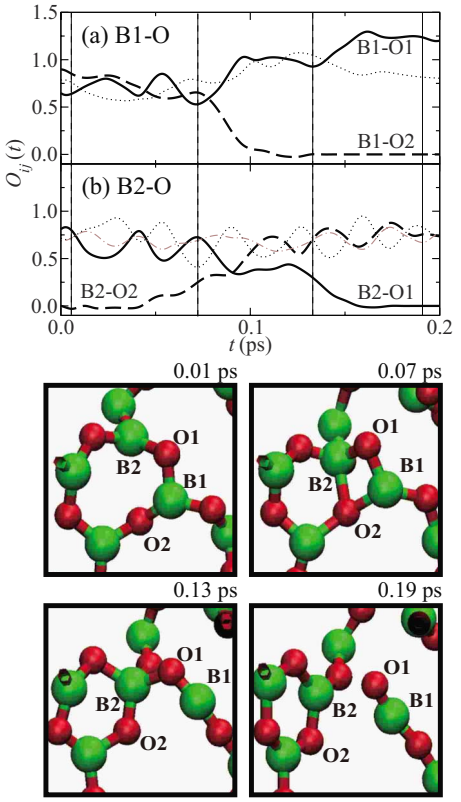

FIG. 6. (Color online) (Top panel) The time evolution of bond-overlap populations $O_{ij}(t)$ for (a) i=B1 and $j \in$ O, and (b) i=B2 and $j \in$ O in the process of the formation of a nonbridging oxygen. The thick solid and thick dashed lines show $O_{ij}(t)$ associated with the B and O atoms of interest. The thin lines show $O_{ij}(t)$ between the B atoms of interest (labeled as "B1" and "B2") and their neighboring O atoms except O1 and O2. (Bottom panel) Atomic configurations at t=0.01, 0.07, 0.13, and 0.19 ps at which the vertical dotted lines are drawn in the top panel. The large and small spheres show B and O atoms, respectively.

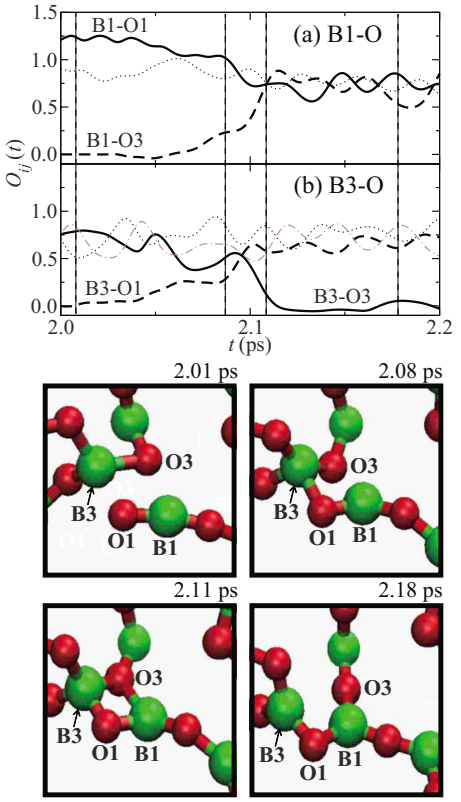

FIG. 7. (Color online) (Top panel) The time evolution of bond-overlap populations $O_{ij}(t)$ for (a) i=B1 and $j \in$ O, and (b) i=B3 and $j \in$ O in the process of the disappearance of the nonbridging oxygen. The thick solid and thick dashed lines show $O_{ij}(t)$ associated with the B and O atoms of interest. The thin lines show $O_{ij}(t)$ between the B atoms of interest (labeled as "B1" and "B3") and their neighboring O atoms except O1 and O3. (Bottom panel) Atomic configurations at t=2.01, 2.08, 2.11, and 2.18 ps at which the vertical dotted lines are drawn in the top panel. The large and small spheres show B and O atoms, respectively.

coordinated, respectively, to heteroatoms, i.e., there is no bond defect. As shown in the top panel of Fig. 6, $O_{B2\text{-}O2}(t)$ begins to increase at about 0.04 ps, which means that a covalent bond is formed between B2 and O2. We can see this new B2-O2 bond in the snapshot at 0.07 ps. Due to the formation of the bond, both B2 and O2 are overcoordinated. Since the overcoordination is energetically unstable, one of the covalent bonds around the threefold-coordinated O2 atom is broken. It is seen that the bond-overlap population between B1 and O2, $O_{B1\text{-}O2}(t)$, becomes almost zero for $t > 0.1$ ps, and the covalent bond between these atoms disappears in the snapshot at 0.13 ps. Note that B1 is coordinated to only two oxygens, while B2 is still overcoordinated. Finally, the covalent bond between B2 and O1 is broken, as $O_{B2\text{-}O1}(t)$ is almost zero for $t > 0.16$ ps. While the threefold coordination of B2 is recovered, O1 is coordinated to only one boron B1, as displayed in the snapshot at 0.19 ps. In this way, the nonbridging O atom (O1) is generated with the twofold-coordinated B atom (B1). We see that there is a double bond between B1 and O1 because $O_{B1\text{-}O1}(t)$ has higher values for $t > 0.16$ ps after the breaking of the B2-O1 bond. It should be noted that this process takes place in the participation of only two overcoordinated (one fourfold-coordinated B and one threefold-coordinated O) atoms, namely, only one BO_4 unit.

After about 2 ps, the double bond between B1 and O1 disappears as shown in Fig. 7. First, the nonbridging O1 approaches B3 to form a new covalent bond between them. We see that $O_{B3\text{-}O1}(t)$ gradually increases for $t > 2.01$ ps as shown in the top panel of Fig. 7 and that O1 is bonded to B3 in the atomic configuration at 2.08 ps. It is also seen that $O_{B1\text{-}O3}(t)$ increases for $t > 2.07$ ps, which means the formation of a covalent bond between B1 and O3 as displayed in the snapshot at 2.11 ps. In this configuration, O1 and B1 have the proper coordination numbers, and instead B3 and O3 are overcoordinated. As $O_{B3\text{-}O3}(t)$ becomes nearly zero at about 2.12 ps, the B3-O3 bond is broken, and an atomic configuration with no bond defect is finally obtained as displayed in the snapshot at 2.18 ps. In this process, two overcoordinated atoms (B3 and O3) are created as in the formation process of the nonbridging O atoms.

Another important diffusion event accompanied by the covalent-bond switching is shown in Fig. 8, where covalent bonds are exchanged around the intermediate defect structure

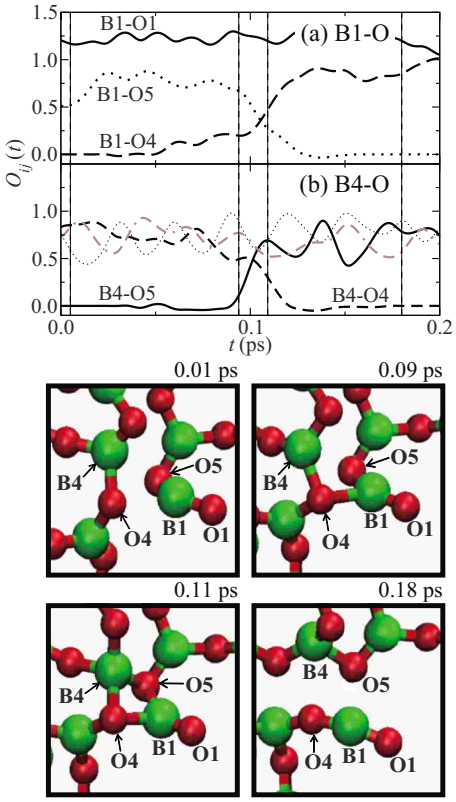

FIG. 8. (Color online) (Top panel) The time evolution of bond-overlap populations $O_{ij}(t)$ for (a) i=B1 and $j \in$ O, and (b) i=B4 and $j \in$ O in a bond-switching process near the nonbridging oxygen. The thick solid, thick dashed, and thick dotted lines show $O_{ij}(t)$ associated with the B and O atoms of interest. The thin lines show $O_{ij}(t)$ between the B atoms of interest (labeled as "B1" and "B4") and their neighboring O atoms except O1, O4, and O5. (Bottom panel) Atomic configurations at t=0.02, 0.09, 0.11, and 0.18 ps at which the vertical dotted lines are drawn in the top panel. The large and small spheres show B and O atoms, respectively.

with the nonbridging O atom while keeping the double bond between the undercoordinated O and B atoms (O1 and B1 in the figure). As seen in the top panel of Fig. 8, around B1 atom, initially $O_{B1\text{-}O4}(t)$ and $O_{B1\text{-}O5}(t)$ are almost zero and finite, respectively, for $t<0.05$ ps, they cross each other at about 0.11 ps, and finally $O_{B1\text{-}O5}(t)$ becomes almost zero, while $O_{B1\text{-}O4}(t)$ is finite for $t>0.14$ ps. This means that a covalent-bond exchange occurs around B1 atom: the covalent bond between B1 and O5 is broken, and at almost the same time a new bond is formed between B1 and O4 (see the atomic configurations in the bottom panel of Fig. 8). In the same say, another covalent-bond exchange occurs around B4 atom: the B4-O4 bond is broken, and the B4-O5 bond is formed, as seen from the time evolution of $O_{B4\text{-}O4}(t)$ and $O_{B4\text{-}O5}(t)$. Note that the coordination number of each atom is unchanged before and after this event. Especially the double bond between B1 and O1 is retained while switching the covalent bonds, as $O_{B1\text{-}O1}(t)$ keeps high values. Since the nonbridging oxygen (O1) is always away from any atoms, it cannot be involved in these concerted bond exchanges.

IV. DISCUSSION

As displayed in Figs. 6 and 7, the B-O bonds are exchanged with the formation of the undercoordinated O and B atoms (O1 and B1) in liquid B_2O_3. It seems to be possible that the covalent bonds are exchanged without the formation of such undercoordinated atoms as in the relaxation process suggested for vitreous B_2O_3.[5] It is, however, necessary to generate two BO_4 groups with sharing two O atoms, namely, four overcoordinated atoms (two overcoordinated B and two overcoordinated O), in this concerted-relaxation process. The energy necessary to create two BO_4 groups is higher than that for the formation process of the nonbridging O atoms, which requires only one BO_4 group as found in our simulations. We consider that this is the reason why most of the diffusion processes take place accompanied by the undercoordinated atoms in liquid B_2O_3.

The intermediate defect structures with the nonbridging O atoms double bonded to twofold-coordinated B atoms are energetically unstable. Therefore they are eventually recovered as shown in Fig. 7. It should be mentioned that the structure of liquid B_2O_3 is rather porous as in solids. Due to the existence of wide void space, the nonbridging oxygens cannot be bonded to other B atoms immediately after their formation. So the nonbridging oxygens diffuse while keeping the double bonds for a period of time, namely, 1.7 ps on average, with the shortest time being 0.8 ps and the longest being 4.3 ps.

Now, we discuss atomic diffusion in liquids with respect to more general aspects of relaxation of local structures. It is known that there exist "cage effects" in metallic[27] and ionic[28] liquids, i.e., atoms or collections of atoms, such as molecules, are surrounded with other atoms or molecules, and exhibit oscillating motion in "cages" formed by the surroundings. When a cage expands sufficiently due to thermal fluctuation, the energy barrier for atoms to escape from the cage becomes lower, and local structural rearrangement (local relaxation) takes place with diffusion of atoms.[29,30] This picture holds for dense liquids in which atoms are densely distributed and the cage around each atom is well defined.

In contrast to these dense liquids, liquid B_2O_3 has void space around each atom. While the repulsive interaction is important to trap atoms in the cage in dense liquids, the covalent bonds play a vital role in capturing atoms in covalent liquids. As was seen in Figs. 6–8, overcoordinated atoms are always generated before atomic diffusion occurs because bond weakening is necessary for the rearrangement of the covalent bonds. Therefore, we can say that the overcoordination is indispensable for diffusion events in covalent liquids. It is seen, from comparison with metallic and ionic liquids described above, that atomic diffusion takes place in different ways depending on the bonding properties of liquids. However, both the cage expansion in dense liquids and the overcoordination in covalent liquids are essentially fluctuations of local density, which is defined as the number of atoms in a given local volume. Hence, the local relaxation accompanying the diffusion of atoms in any kind of liquid is commonly understood in the sense that thermally induced local-density fluctuations are always required for structural-rearrangement events.

Since the local-density fluctuations become larger at higher temperatures, the number of diffusion events increases in most liquids in response to an increase in temperature. In contrast, the effects of pressure are not simple. Although the structural rearrangement is usually expected to be suppressed in liquids under pressure, some covalent liquids have a maximum in the pressure dependence of the diffusivity.[31] It can be imagined that bond weakening occurs in covalent liquids under pressure due to an increase in the coordination numbers, which suggests that atoms diffuse more easily with increasing pressure. When the pressure is further increased, the covalent nature will eventually be lost, and the average coordination number will approach those of dense liquids. The cage effects should be dominant even in covalent liquids under such high pressures, and the diffusivity will decrease with pressure. It would be worthwhile to confirm this scenario in liquid B_2O_3 by investigating the effects of pressure on the dynamic properties.

V. SUMMARY

The microscopic mechanism of atomic diffusion in liquid B_2O_3 has been investigated by *ab initio* molecular dynamics simulations. It has been confirmed that, even in the liquid state, boron and oxygen atoms are predominantly threefold- and twofold-coordinated, respectively, to heteroatoms with single covalent bond, as in the crystalline and vitreous states. We have found that there appears a nonbridging oxygen double bonded to a twofold-coordinated boron whenever atomic diffusion occurs accompanied by the covalent-bond exchanges. The formation mechanism of such defect structure with the nonbridging oxygen has been discussed in detail using the time evolution of the bond-overlap populations between atoms. We have demonstrated that the covalent bonds can be exchanged around the defect structures while keeping the double bonds between the undercoordinated atoms before the bond defects are recovered.

ACKNOWLEDGMENTS

The authors acknowledge useful discussions with Masaru Aniya. The present work was supported in part by a Grant-in-Aid for Scientific Research on Priority Area, Nanoionics (439) from MEXT, Japan. The authors thank the Supercomputer Center, Institute for Solid State Physics, University of Tokyo for the use of facilities. The computation was also carried out using the computer facilities at Research Institute for Information Technology, Kyushu University.

[1] G. E. Gurr, P. W. Montgomery, C. D. Knutson, and B. T. Gorres, Acta Crystallogr., Sect. B: Struct. Crystallogr. Cryst. Chem. **26**, 906 (1970).
[2] P. A. V. Johnson, A. C. Wright, and R. N. Sinclair, J. Non-Cryst. Solids **50**, 281 (1982).
[3] J. Sakowski and G. Herms, J. Non-Cryst. Solids **293-295**, 304 (2001).
[4] A. S. Zyubin, S. A. Dembovsky, and O. A. Kondakova, J. Non-Cryst. Solids **224**, 291 (1998).
[5] J. Kieffer, Phys. Rev. B **50**, 17 (1994).
[6] J. Diefenbacher and P. F. McMillan, J. Phys. Chem. A **105**, 7973 (2001).
[7] T. Koishi and M. Misawa, J. Phys. Soc. Jpn. **68**, 2669 (1999).
[8] A. Takada, C. R. A. Catlow, J. S. Lin, G. D. Price, M. H. Lee, V. Milman, and M. C. Payne, Phys. Rev. B **51**, 1447 (1995).
[9] D. Li and W. Y. Ching, Phys. Rev. B **54**, 13616 (1996).
[10] U. Engberg, Phys. Rev. B **55**, 2824 (1997).
[11] M. M. Islam, T. Bredow, and C. Minot, Chem. Phys. Lett. **418**, 565 (2006).
[12] T. Uchino and T. Yoko, J. Chem. Phys. **105**, 4140 (1996).
[13] P. Umari and A. Pasquarello, Phys. Rev. Lett. **95**, 137401 (2005).
[14] V. V. Brazhkin, Y. Katayama, K. Trachenko, O. B. Tsiok, A. G. Lyapin, E. Artacho, M. Dove, G. Ferlat, Y. Inamura, and H. Saitoh, Phys. Rev. Lett. **101**, 035702 (2008).
[15] P. E. Blöchl, Phys. Rev. B **50**, 17953 (1994).
[16] G. Kresse and D. Joubert, Phys. Rev. B **59**, 1758 (1999).
[17] J. P. Perdew, K. Burke, and M. Ernzerhof, Phys. Rev. Lett. **77**, 3865 (1996).
[18] G. Kresse and J. Hafner, Phys. Rev. B **49**, 14251 (1994).
[19] F. Shimojo, R. K. Kalia, A. Nakano, and P. Vashishta, Comput. Phys. Commun. **140**, 303 (2001).
[20] S. Nosé, Mol. Phys. **52**, 255 (1984).
[21] W. G. Hoover, Phys. Rev. A **31**, 1695 (1985).
[22] M. Tuckerman, B. J. Berne, and G. J. Martyna, J. Chem. Phys. **97**, 1990 (1992).
[23] P. B. Macedo, W. Capps, and T. A. Litovitz, J. Chem. Phys. **44**, 3357 (1966).
[24] A. C. Hannon, D. I. Grimley, R. A. Hulme, A. C. Wright, and R. N. Sinclair, J. Non-Cryst. Solids **177**, 299 (1994).
[25] R. S. Mulliken, J. Chem. Phys. **23**, 1833 (1955); **23**, 1841 (1955).
[26] F. Shimojo, A. Nakano, R. K. Kalia, and P. Vashishta, Phys. Rev. E **77**, 066103 (2008).
[27] F. Shimojo, Y. Zempo, K. Hoshino, and M. Watabe, Phys. Rev. B **52**, 9320 (1995).
[28] T. J. Chuang, G. W. Hoffman, and K. B. Eisenthal, Chem. Phys. Lett. **25**, 201 (1974).
[29] J. C. Dyre, Rev. Mod. Phys. **78**, 953 (2006).
[30] K. Trachenko, J. Non-Cryst. Solids **354**, 3903 (2008).
[31] S. Tsuneyuki and Y. Matsui, Phys. Rev. Lett. **74**, 3197 (1995).